

Scalable Gaussian Process Computations Using Hierarchical Matrices

Christopher J. Geoga *

Mathematics and Computer Science Division, Argonne National Laboratory

Mihai Anitescu †

Mathematics and Computer Science Division, Argonne National Laboratory

Department of Statistics, University of Chicago

Michael L. Stein ‡

Department of Statistics, University of Chicago

Abstract

We present a kernel-independent method that applies hierarchical matrices to the problem of maximum likelihood estimation for Gaussian processes. The proposed approximation provides natural and scalable stochastic estimators for its gradient and Hessian, as well as the expected Fisher information matrix, that are computable in quasilinear $O(n \log^2 n)$ complexity for a large range of models. To accomplish this, we (i) choose a specific hierarchical approximation for covariance matrices that enables the computation of their exact derivatives and (ii) use a stabilized form of the Hutchinson stochastic trace estimator. Since both the observed and expected information matrices can be computed in quasilinear complexity, covariance matrices for MLEs can also be estimated efficiently. After discussing the associated mathematics, we demonstrate the scalability of the method, discuss details of its implementation, and validate that the resulting MLEs and confidence intervals based on the inverse Fisher information matrix faithfully approach those obtained by the exact likelihood.

Keywords: Algorithms, Numerical Linear Algebra, Spatial Analysis, Statistical Computing

*corresponding author: cgeoga@anl.gov

†This material was based upon work supported by the U.S. Department of Energy, Office of Science, Office of Advanced Scientific Computing Research (ASCR) under Contract DE-AC02-06CH11347. We acknowledge partial NSF funding through awards FP061151-01-PR and CNS-1545046 to MA.

‡This material was based upon work supported by the U.S. Department of Energy, Office of Science, Office of Advanced Scientific Computing Research (ASCR) under Contract DE-AC02-06CH11357.

1 Introduction

Many real-valued stochastic processes $Z(\mathbf{x})$, $\mathbf{x} \in \mathbb{R}^d$, are modeled as Gaussian processes, so that observing $Z(\mathbf{x})$ at locations $\{\mathbf{x}_j\}_{j=1}^n$ results in the data $\mathbf{y} \in \mathbb{R}^n$ following a $N(\boldsymbol{\mu}, \boldsymbol{\Sigma})$ distribution. Here the covariance matrix $\boldsymbol{\Sigma}$ is parameterized by a valid covariance function $K(\cdot, \cdot; \boldsymbol{\theta})$ that depends on parameters $\boldsymbol{\theta} \in \mathbb{R}^m$, so that

$$\begin{aligned}\boldsymbol{\Sigma}_{j,k} &= \text{Cov}(Z(\mathbf{x}_j), Z(\mathbf{x}_k)) \\ &= K(\mathbf{x}_j, \mathbf{x}_k; \boldsymbol{\theta}), \quad j, k = 1, 2, \dots, n.\end{aligned}$$

In many cases in the physical sciences, estimating the parameters $\boldsymbol{\theta}$ is of great practical and scientific interest. The reference tool to estimate $\boldsymbol{\theta}$ given data \mathbf{y} is the *maximum likelihood estimator* (MLE), which is the vector $\hat{\boldsymbol{\theta}}$ that minimizes the negative log-likelihood, given by

$$-l(\boldsymbol{\theta}) := \frac{1}{2} \log |\boldsymbol{\Sigma}(\boldsymbol{\theta})| + \frac{1}{2}(\mathbf{y} - \boldsymbol{\mu})^T \boldsymbol{\Sigma}(\boldsymbol{\theta})^{-1}(\mathbf{y} - \boldsymbol{\mu}) + \frac{n}{2} \log(2\pi). \quad (1)$$

For a detailed discussion of maximum likelihood and estimation methods, see Stein (1999). In our discussions here of the log-likelihood, the mean vector $\boldsymbol{\mu}$ will be assumed to be zero, and the constant term will be suppressed. Also, for notational simplicity, the explicit dependence of $\boldsymbol{\Sigma}$ on $\boldsymbol{\theta}$ will not be indicated in the rest of this paper.

From a computational perspective, finding the minimizer of (1) can be challenging. The immediate difficulty is that the linear algebraic operations required to evaluate (1) grow with cubic time complexity. Thus, as the data size n increases, direct evaluation of the log-likelihood quickly becomes prohibitively slow. Further, the storage complexity associated with evaluating (1) grows quadratically, so storing $\boldsymbol{\Sigma}$ in memory can rapidly become infeasible if the kernel $K(\cdot, \cdot)$ is not compactly supported. For example, even for a moderate $n = 2^{15}$, storing $\boldsymbol{\Sigma}$ requires more than 8 GB of memory, which may require careful storage management even on modern workstations.

As a result of these difficulties, many methods have been proposed that improve both the time and memory complexity of evaluating or approximating (1) as well as finding its minimizer in indirect ways. Perhaps the oldest systematic methods for the fast approximation of the likelihood are the “composite methods,” which can loosely be thought of in this context as a block-sparse approximation of $\boldsymbol{\Sigma}$ (Vecchia 1988, Stein et al. 2004, Caragea & Smith 2007, Katzfuss 2017, Katzfuss & Guinness 2018). In a different approach, the methods of matrix tapering (Furrer et al. 2006, Kaufman et al. 2008, Castrillon-Candas et al. 2016) and Markov random fields (Rue & Held 2005, Lindgren et al. 2011) use approximations that induce sparsity in $\boldsymbol{\Sigma}$, facilitating linear algebra with better scaling that way. Approximations of $\boldsymbol{\Sigma}$ as a low-rank update to a diagonal matrix have also been applied to this problem (Cressie & Johannesson 2006), although they can perform poorly in some settings (Stein 2014). In a different approach, by side-stepping the likelihood entirely and instead solving estimating equations (Godambe 1991, Heyde 2008), one can avoid log-determinant computation and perform a smaller set of linear algebraic operations that are

more easily accelerated, potentially approximating MLEs with only matrix-vector products $\Sigma \mathbf{x}$ if iterative solvers are used (Anitescu et al. 2011, Stein et al. 2013, Sun & Stein 2016).

The estimating equations approach involves solving a nonlinear system of equations that in the case of the score equations are given by

$$-\nabla l(\boldsymbol{\theta})_j := \frac{1}{2} \text{tr}(\Sigma^{-1} \Sigma_j) - \frac{1}{2} \mathbf{y}^T \Sigma^{-1} \Sigma_j \Sigma^{-1} \mathbf{y}, \quad (2)$$

where here and throughout the paper Σ_j denotes $\frac{\partial}{\partial \theta_j} \Sigma(\boldsymbol{\theta})$. The primary difficulty with computing these expressions is that the trace of the matrix-matrix product $\Sigma^{-1} \Sigma_j$ is prohibitively expensive to compute exactly. To get around this, Anitescu et al. (2011) proposed using sample average approximation (SAA), which utilizes the unbiased stochastic trace estimator proposed by Hutchinson (1990). For (2) it is given by

$$\frac{1}{N_h} \sum_{l=1}^{N_h} \mathbf{u}_l^T \Sigma^{-1} \Sigma_j \mathbf{u}_l,$$

where the stochastic \mathbf{u}_l are symmetric Bernoulli vectors (although other options are available; see Stein et al. (2013) for details). Stein et al. (2013) notes that if it is feasible to compute a symmetric factorization $\Sigma = \mathbf{W} \mathbf{W}^T$, then there may be advantages to using a “symmetrized” trace estimator

$$\frac{1}{N_h} \sum_{l=1}^{N_h} \mathbf{u}_l^T \mathbf{W}^{-1} \Sigma_j \mathbf{W}^{-T} \mathbf{u}_l.$$

Specifically, writing \mathcal{I} for the expected Fisher information matrix, Stein et al. (2013) shows that the covariance matrix of these estimates is bounded by $(1 + \frac{1}{N_h})\mathcal{I}$, whereas if we do not symmetrize, Stein et al. (2013) gives the bound $(1 + \frac{(\kappa+1)^2}{4N_h\kappa})\mathcal{I}$, where κ is the condition number of the covariance matrix at the true parameter value. Since $\kappa \geq 1$, the bound with symmetrization is at least as small as the bound without it. Of course, this does not prove that the actual covariance matrix is smaller, but the results in Section 4 show that the improvement due to symmetrization can be large. Moreover, the symmetrized trace estimator reduces the number of linear solves from two to one if $\Sigma^{-1} \mathbf{y}$ is computed as $\mathbf{W}^{-T} \mathbf{W}^{-1} \mathbf{y}$, saving computer time.

Recently, significant effort has been expended to apply the framework of hierarchical matrices (Hackbusch 1999, Grasedyck & Hackbusch 2003, Hackbusch 2015)—which utilize the low-rank block structure of certain classes of special matrices to obtain significantly better time and storage complexity for common operations—to the problem of Gaussian process computing (Börm & Garcke 2007, Ambikasaran et al. 2016, Minden et al. 2017, Litvinenko et al. 2017, Chen & Stein 2017). We follow in this vein here, extending some of these ideas by using the specific class of hierarchical matrices referred to as hierarchical off-diagonal low-rank (HODLR) matrices (Ambikasaran & Darve 2013). Unlike some of the methods described earlier, approaches to approximating l_H with hierarchical matrices

have the benefit of being able to directly compute the log-determinant of Σ and the linear solve $\Sigma^{-1}\mathbf{y}$. Letting $\tilde{\Sigma}$ denote a hierarchical approximation of Σ here and throughout the paper, we give the approximated log-likelihood as

$$-l_H(\boldsymbol{\theta}) := \frac{1}{2} \log |\tilde{\Sigma}| + \frac{1}{2} \mathbf{y}^T \tilde{\Sigma}^{-1} \mathbf{y}. \quad (3)$$

While the issue of how well $\tilde{\Sigma}$ approximates Σ remains, the applications of H-matrices to maximum likelihood cited above have demonstrated that such approximations for covariance matrices can yield good estimates of $\hat{\boldsymbol{\theta}}$.

Most investigations into the use of hierarchical matrices in this area focus exclusively on the computation of $l_H(\boldsymbol{\theta})$, and not, for example, its first- and second-order derivatives. If the goal is to carry out minimization of $-l_H(\boldsymbol{\theta})$, however, access to such information would significantly reduce the number of iterations required to approximate $\hat{\boldsymbol{\theta}}$ (Nocedal & Wright 2006). Part of the difficulty is that the matrix product $\tilde{\Sigma}^{-1} \tilde{\Sigma}_j$ is still expensive to compute for hierarchical matrices, and so the trace term in the score equations is still challenging to obtain quickly. As a result, stochastic methods for estimating the trace associated with the gradient of l_H are still necessary in order to maintain good complexity. An alternative method to the Hutchinson estimator is suggested by Minden et al. (2017), who utilize the peeling algorithm of Lin et al. (2011) to assemble a hierarchical approximation of $\tilde{\Sigma}^{-1} \tilde{\Sigma}_j$ and obtain a more precise estimate for its trace. In this setting especially, however, this is done at the cost of substantially higher overhead than occurs with the Hutchinson estimator. As is demonstrated in this paper, the symmetrized Hutchinson estimator is reliable enough for the purpose of numerical optimization.

One important choice for the construction of hierarchical approximations is the method for compressing low-rank off-diagonal blocks; we refer readers to Ambikasaran et al. (2016) for a discussion. In this work, we advocate the use of the Nyström approximation (Williams & Seeger 2001, Drineas & Mahoney 2005, Chen & Stein 2017). The Nyström approximation of the block of Σ corresponding to indices I and J is given by

$$\tilde{\Sigma}_{I,J} := \Sigma_{I,P} \Sigma_{P,P}^{-1} \Sigma_{P,J}, \quad (4)$$

where the indices P are for p many *landmark points* that are chosen from the dataset. As can be seen, this formulation is less natural to use in an adaptive way than, for example, a truncated singular value decomposition or other common fast approximation methods. Unlike most adaptive methods (Griewank & Walther 2008), however, it is differentiable with respect to the parameters $\boldsymbol{\theta}$, a property that is essential to the approach advocated here. As a result of this unique property, the derivatives of $\tilde{\Sigma}(\boldsymbol{\theta})$ are both well defined and computable in quasilinear complexity if its off-diagonal blocks are constructed with the Nyström approximation. This means that the second term in (2), which has sequential solves and matrix-vector products with the derivative matrix $\tilde{\Sigma}_j$, can be computed exactly.

In this paper, we discuss an approach to minimizing (3) that combines the HODLR matrix structure from Ambikasaran & Darve (2013), the Nyström approximation of Williams & Seeger (2001), and the sample average (SAA) trace estimation from Anitescu et al.

(2011) and Stein et al. (2013) in its symmetrized form. As a result, we obtain stable and optimization-suitable stochastic estimates for the gradient and Hessian of (3) in quasilinear time and storage complexity at a comparatively low overhead. Combined with the exact derivatives of $\tilde{\Sigma}$, the symmetrized stochastic trace estimators are demonstrated to yield gradient and Hessian approximations with relative numerical error below 0.03% away from the MLE for a manageably small number of \mathbf{u}_l vectors. As well as providing tools for optimization, the exact first derivatives and stabilized trace estimation mean that the observed and expected Fisher information matrix may be computed in quasilinear complexity, serving as a valuable tool for estimating the covariance matrix of $\hat{\theta}$, which is often of great scientific interest as well.

1.1 Comparison with existing methods

Like the works of Börm & Garcke (2007), Anitescu et al. (2011), Stein et al. (2013), Minden et al. (2017), Litvinenko et al. (2017), and Chen & Stein (2017), we attempt to provide an approximation of the log-likelihood that can be computed with good efficiency but whose minimizers closely resemble those of the exact likelihood. The primary distinction between our approach and other methods is that we construct our approximation with an emphasis on having mathematically well-defined and computationally feasible first and second derivatives. By computing the exact derivative of the approximation of Σ , given by $\tilde{\Sigma}_j = \frac{\partial}{\partial \theta_j} \tilde{\Sigma}$, instead of the independent approximation of the derivative of the exact Σ , which might be denoted by $\widetilde{\frac{\partial}{\partial \theta_j} \Sigma}$ to emphasize that one is approximating the derivative of the exact matrix $\Sigma(\theta)$, we obtain a much more coherent framework for thinking about both optimization and error propagation in the derivatives of l_H . As an example of the practical significance of this distinction, for a scale parameter θ_0 and covariance matrix parameterized with $\tilde{\Sigma} = \theta_0 \tilde{\Sigma}'$, the derivative $\frac{\partial}{\partial \theta_0} \tilde{\Sigma}$ will be numerically identical to $\tilde{\Sigma}'$, making $\tilde{\Sigma}^{-1} \tilde{\Sigma}_j$ an exact rescaled identity matrix. As a result, the stochastic Hutchinson trace estimator of that matrix-matrix product for scale parameters is exact to numerical precision with a single \mathbf{u}_l , which will be reflected in the numerical results section. To our knowledge, such a guarantee cannot be made if $\tilde{\Sigma}_j$ is constructed as an approximation of the exact derivative Σ_j . Moreover, none of the methods mentioned above discuss computing Hessian information of any kind.

Our approach achieves quasilinear complexity both in evaluating the log-likelihood and in computing accurate and stable stochastic estimators for the gradient and Hessian of the approximated log-likelihood. This comes at the cost of abandoning a priori controllable bounds on pointwise precision of the hierarchical approximation of the exact covariance matrix, a less accurate trace estimator than has been achieved with the peeling method (Minden et al. 2017, Lin et al. 2011), and sub-optimal time and storage complexity (Chen & Stein 2017). Nevertheless, we consider this to be a worthwhile tradeoff in some applications, and we demonstrate in the numerical results section that despite the loss of control of pointwise error in the covariance, we can compute estimates for MLEs and their

corresponding uncertainties from the expected Fisher matrix that agree well with exact methods. Further, by having access to a scalable gradient and Hessian, we have many options for numerical optimization and are able to perform such optimization reliably and efficiently.

2 HODLR matrices, derivatives, and trace estimation

In this study, we approximate Σ with the HODLR format (Ambikasaran & Darve 2013), which has an especially simple and tractable structure given by

$$\begin{bmatrix} \mathbf{A}_1 & \mathbf{U}\mathbf{V}^T \\ \mathbf{V}\mathbf{U}^T & \mathbf{A}_2 \end{bmatrix}, \quad (5)$$

where the matrices \mathbf{U} and \mathbf{V} are of dimension $n \times p$ and \mathbf{A}_1 and \mathbf{A}_2 are either dense matrices or are of the form of (5) themselves. A matrix of size $n \times n$ can be split recursively into block 2×2 matrices in this way $\lfloor \log_2(n) \rfloor$ times, although in practice it is often divided fewer times than that. The diagonal blocks of a HODLR matrix are often referred to as the *leaves*, referring to the fact that a tree is implicitly being constructed. For a visual example, a HODLR matrix of “level” 2 may look like

$$\begin{bmatrix} \begin{bmatrix} \mathbf{L}_1 & \mathbf{U}_{11}\mathbf{V}_{11}^T \\ \mathbf{V}_{11}\mathbf{U}_{11}^T & \mathbf{L}_2 \end{bmatrix} & \mathbf{U}_{01}\mathbf{V}_{01}^T \\ \mathbf{V}_{01}\mathbf{U}_{01}^T & \begin{bmatrix} \mathbf{L}_3 & \mathbf{U}_{12}\mathbf{V}_{12}^T \\ \mathbf{V}_{12}\mathbf{U}_{12}^T & \mathbf{L}_4 \end{bmatrix} \end{bmatrix}.$$

Symmetric positive definite HODLR matrices admit an exact symmetric factorization $\tilde{\Sigma} = \mathbf{W}\mathbf{W}^T$ that can be computed in $O(n \log^2 n)$ complexity if p is fixed and the level grows with $O(\log n)$ (Ambikasaran et al. 2016). For a matrix of level τ , \mathbf{W} takes the form

$$\mathbf{W} = \overline{\mathbf{W}} \prod_{k=1}^{\tau} \left\{ \mathbb{I} + \overline{\mathbf{U}}_k \overline{\mathbf{V}}_k^T \right\},$$

where $\overline{\mathbf{W}}$ is a block-diagonal matrix of the symmetric factors of the leaves \mathbf{L}_k and each $\mathbb{I} + \overline{\mathbf{U}} \overline{\mathbf{V}}^T$ is a block-diagonal low-rank update to the identity.

If the rank of the off-diagonal blocks is fixed at p and the level grows with $O(\log n)$, then the log-determinant and linear system computations can both be performed at $O(n \log n)$ complexity by using the symmetric factor (Ambikasaran et al. 2016). With these tools, we may evaluate the approximated Gaussian log-likelihood given in (3) exactly and directly. We note that the assembly of the matrix and its factorization are parallelizable and that many of the computations in the numerical results section are done in single-node multicore parallel.

2.1 The Nyström approximation and gradient estimation

As mentioned in the Introduction, the method we advocate here for the low-rank compression of off-diagonal blocks is the Nyström approximation (Williams & Seeger 2001), a method recently applied to Gaussian process computing and hierarchical matrices (Chen & Stein 2017). Unlike the multiple common algebraic approximation methods that often construct approximations of the form \mathbf{UV}^T by imitating early-terminating pivoted factorization (Ambikasaran et al. 2016), for example the commonly used adaptive cross-approximation (ACA) (Bebendorf 2000, Rjasanow 2002), the Nyström approximation constructs approximations that are continuous with respect to the parameters $\boldsymbol{\theta}$ in a nonadaptive way. Another advantage of this method is that an approximation $\tilde{\boldsymbol{\Sigma}}$ assembled with the Nyström approximation is guaranteed to be positive definite if $\boldsymbol{\Sigma}$ is (Chen & Stein 2017), avoiding the common difficulty of guaranteeing that a hierarchical approximation $\tilde{\boldsymbol{\Sigma}}$ of positive definite $\boldsymbol{\Sigma}$ is itself positive definite (Bebendorf & Hackbusch 2007, Xia & Gu 2010, Chen & Stein 2017).

The cost of choosing the Nyström approximation for off-diagonal blocks instead of a method like the ACA is that we cannot easily adapt it locally to a prescribed accuracy. That is, constructing a factorization with a precision ε so that $\|\boldsymbol{\Sigma}_{I,J} - \tilde{\boldsymbol{\Sigma}}_{I,J}\| < \varepsilon \|\boldsymbol{\Sigma}_{I,J}\|$ is difficult since we must choose the number and locations of the landmark points P before starting computations. Further, the number and locations of the landmark points are global for the whole matrix, so an adaptive algorithm that approximates some blocks as having higher ranks in order to control precision for the whole matrix is not available in this framework.

The primary appeal of this approximation for our purposes, however, is that its derivatives exist and are readily computable by the product rule, given by

$$\tilde{\boldsymbol{\Sigma}}_{j,(I,J)} = \boldsymbol{\Sigma}_{j,(I,P)} \boldsymbol{\Sigma}_{P,P}^{-1} \boldsymbol{\Sigma}_{P,J} - \boldsymbol{\Sigma}_{I,P} \boldsymbol{\Sigma}_{P,P}^{-1} \boldsymbol{\Sigma}_{j,(P,P)} \boldsymbol{\Sigma}_{P,P}^{-1} \boldsymbol{\Sigma}_{P,J} + \boldsymbol{\Sigma}_{I,P} \boldsymbol{\Sigma}_{P,P}^{-1} \boldsymbol{\Sigma}_{j,(P,J)}, \quad (6)$$

where, for example, $\boldsymbol{\Sigma}_{j,(I,J)} = \frac{\partial}{\partial \boldsymbol{\theta}_j} \boldsymbol{\Sigma}_{I,J}$, with parentheses and capitalization used to emphasize subscripts denoting block indices. Fortunately, all three terms in (6) are the product of $n \times p$ and $p \times p$ matrices. Since the diagonal blocks of $\tilde{\boldsymbol{\Sigma}}_j$ are trivially computable as well, the exact derivative of $\tilde{\boldsymbol{\Sigma}}$ can be represented as a HODLR matrix with the same shape as $\tilde{\boldsymbol{\Sigma}}$ except that now the off-diagonal blocks are sums of three terms that look like truncated factorizations of the form \mathbf{USV}^T , where $\mathbf{S} \in \mathbb{R}^{p \times p}$. In practice, assembling and storing $\tilde{\boldsymbol{\Sigma}}_j$ take only about twice as much time and memory as required for $\tilde{\boldsymbol{\Sigma}}$. This feature is convenient for computing the gradient of the approximated log-likelihood for Gaussian processes, since in this setting one can compute terms of the form $\mathbf{y}^T \tilde{\boldsymbol{\Sigma}}^{-1} \tilde{\boldsymbol{\Sigma}}_j \tilde{\boldsymbol{\Sigma}}^{-1} \mathbf{y}$ exactly and in the same quasilinear time and storage complexity.

We now combine our results from the preceding section with the symmetrized trace estimation discussed in the Introduction and obtain a stochastic gradient approximation for $-l_H$ that can be computed in quasilinear complexity:

$$\nabla \widehat{-l_H}(\boldsymbol{\theta})_j = \frac{1}{2N_h} \sum_{l=1}^{N_h} \mathbf{u}_l^T \mathbf{W}^{-1} \tilde{\boldsymbol{\Sigma}}_j \mathbf{W}^{-T} \mathbf{u}_l - \frac{1}{2} \mathbf{y}^T \tilde{\boldsymbol{\Sigma}}^{-1} \tilde{\boldsymbol{\Sigma}}_j \tilde{\boldsymbol{\Sigma}}^{-1} \mathbf{y}.$$

Both the symmetrized trace estimator, facilitated by the symmetric factorization, and the exact derivatives, facilitated by the Nyström approximation, are important to the performance of this estimator. While the benefit of the latter is clear, the decreased variance and faster computation time are nontrivial benefits as well. The numerical results section has a brief demonstration of these benefits.

2.2 Stochastic estimation of information matrices

Being able to efficiently and effectively estimate trace terms involving the derivatives $\tilde{\Sigma}_j$ also facilitates accurate estimation of the expected Fisher information matrix, which has terms given by

$$\mathcal{I}_{j,k} = \frac{1}{2} \text{tr} \left(\tilde{\Sigma}^{-1} \tilde{\Sigma}_j \tilde{\Sigma}^{-1} \tilde{\Sigma}_k \right).$$

Using the same symmetrization approach as above, we may compute stochastic estimates of these terms with the unbiased and fully symmetrized estimator

$$\hat{\mathcal{I}}_{j,j} + \hat{\mathcal{I}}_{k,k} + 2\hat{\mathcal{I}}_{j,k} = \frac{1}{2N_h} \sum_{l=1}^{N_h} \mathbf{u}_l^T \mathbf{W}^{-1} \left(\tilde{\Sigma}_j + \tilde{\Sigma}_k \right) \tilde{\Sigma}^{-1} \left(\tilde{\Sigma}_j + \tilde{\Sigma}_k \right) \mathbf{W}^{-T} \mathbf{u}_l. \quad (7)$$

Since the diagonal elements of $\hat{\mathcal{I}}$ can be computed first in a simple and trivially symmetric way, this provides a fully symmetrized method for estimating $\mathcal{I}_{j,k}$. Further, computing the estimates in the form of (7) does not require any more matvec applications of derivative matrices than would the more direct estimator that computes terms as $\mathbf{u}_l^T \mathbf{W}^{-1} \tilde{\Sigma}_j \tilde{\Sigma}^{-1} \tilde{\Sigma}_k \mathbf{W}^{-T} \mathbf{u}_l$, since the terms in (7) look like $\mathbf{u}^T \mathbf{A} \mathbf{A}^T \mathbf{u} = \|\mathbf{A}^T \mathbf{u}\|^2$, if we recall that the innermost solve $\tilde{\Sigma}^{-1} \mathbf{y}$ is computed by sequential solves $\mathbf{W}^{-T} \mathbf{W}^{-1} \mathbf{y}$. As a result, each term in (7) still requires only one full solve with $\tilde{\Sigma}$ and two derivative matrix applications.

Having efficient and accurate estimates for $\mathcal{I}(\boldsymbol{\theta})$ is helpful because they can be used for confidence intervals, since asymptotic theory suggests (Stein 1999) that if the smallest eigenvalue of \mathcal{I} tends to infinity as the sample size increases, then we can expect that

$$\mathcal{I}(\hat{\boldsymbol{\theta}})^{1/2} (\hat{\boldsymbol{\theta}} - \boldsymbol{\theta}_{\text{true}}) \rightarrow_D N(0, \mathbb{I}).$$

The Hessian of $-l_H$, which requires computing second derivatives of $\tilde{\Sigma}$, is useful for both optimization and inference. The exact terms of the Hessian $(Hl_H)_{j,k}$ are given by

$$\frac{1}{2} \left(-\text{tr} \left(\tilde{\Sigma}^{-1} \tilde{\Sigma}_k \tilde{\Sigma}^{-1} \tilde{\Sigma}_j \right) + \text{tr} \left(\tilde{\Sigma}^{-1} \tilde{\Sigma}_{jk} \right) \right) - \frac{1}{2} \mathbf{y}^T \left(\frac{\partial}{\partial \theta_k} \tilde{\Sigma}^{-1} \tilde{\Sigma}_j \tilde{\Sigma}^{-1} \right) \mathbf{y}, \quad (8)$$

where

$$\frac{\partial}{\partial \theta_k} \tilde{\Sigma}^{-1} \tilde{\Sigma}_j \tilde{\Sigma}^{-1} = -\tilde{\Sigma}^{-1} \tilde{\Sigma}_k \tilde{\Sigma}^{-1} \tilde{\Sigma}_j \tilde{\Sigma}^{-1} + \tilde{\Sigma}^{-1} \tilde{\Sigma}_{jk} \tilde{\Sigma}^{-1} - \tilde{\Sigma}^{-1} \tilde{\Sigma}_j \tilde{\Sigma}^{-1} \tilde{\Sigma}_k \tilde{\Sigma}^{-1}.$$

Continuing further with the symmetrization approach, we obtain the unbiased fully symmetrized stochastic estimator of the first two terms of (8) given by

$$\frac{1}{2N_h} \sum_{l=1}^{N_h} \mathbf{u}_l^T \mathbf{W}^{-1} \tilde{\Sigma}_{jk} \mathbf{W}^{-T} \mathbf{u}_l - \hat{\mathcal{I}}_{j,k},$$

where $\widehat{\mathcal{I}}_{j,k}$ is the j, k th term of the estimated Fisher information matrix.

Since the third and fourth terms in (8) can be computed exactly, replacing the two trace terms in (8) with the stochastic trace estimator provides a stochastic approximation for the Hessian of $-l_H$. The computation of the second partial derivatives $\widetilde{\Sigma}_{jk}$ is a straightforward continuation of the computations of Equation (6) and will again result in the sum of a small number of HODLR matrices with the same structure. The overall effort of estimating the Hessian of (3) with our approach will thus also have $O(n \log^2 n)$ complexity, providing extra tools for both optimization and covariance matrix estimation, since in some circumstances the observed information is a preferable estimator to the expected information (Efron & Hinkley 1978). We note, however, that our approximation of the expected Fisher information is guaranteed to be positive semidefinite if one uses the same \mathbf{u}_l vectors for all components of the matrix, whereas our approximation of the Hessian may not be positive semidefinite at the MLE. Because of their length, exact expressions for $\widetilde{\Sigma}_{jk}$ have been left to the Appendix.

3 Numerical results

We now present several numerical experiments to demonstrate both the accuracy and scalability of the proposed approximation to the log-likelihood for Gaussian process data. In the sections below, we demonstrate the effectiveness of this method using two parameterizations of the Matérn covariance, which is given in its most standard form by

$$K(\mathbf{x}, \mathbf{y}; \boldsymbol{\theta}, \nu) := \theta_0 \mathcal{M}_\nu \left(\frac{\|\mathbf{x} - \mathbf{y}\|}{\theta_1} \right). \quad (9)$$

Here, \mathcal{M}_ν is the Matérn correlation function, given by

$$\mathcal{M}_\nu(x) := (2^{\nu-1} \Gamma(\nu))^{-1} (\sqrt{2\nu} x)^\nu \mathcal{K}_\nu(\sqrt{2\nu} x),$$

and \mathcal{K}_ν is the modified Bessel function of the second kind. The quantity θ_0 is a scale parameter, θ_1 is a range parameter, and ν is a smoothness parameter that controls the degree of differentiability if the process is differentiable or, equivalently, the high-frequency behavior of the spectral density (Stein 1999).

As well as demonstrating the similar behavior of the exact likelihood to the approximation we present, this section explores the important algorithmic choices that can be tuned or selected. These are (i) the number of block-dyadic divisions of the matrix (the *level* of the HODLR matrix) and (ii) the globally fixed *rank* of the off-diagonal blocks. These choices are of particular interest in addressing possible concerns that the resulting estimate from minimizing $-l_H$ may be sensitive to the choices of these parameters and that choosing reasonable a priori values may be difficult, although we demonstrate below that the method is relatively robust to these choices.

In all the numerical simulations and studies described below, unless otherwise stated, the fixed rank of off-diagonal blocks has been set at 72 and the HODLR level at $\lfloor \log_2 n \rfloor - 8$,

which results in diagonal blocks (leaves) with sizes between 256 and 512. The ordering of the observations/spatial locations is done through the traversal of a K-D tree as in Ambikasaran et al. (2016), which is a straightforward extension to the familiar one-dimensional tree whose formalism is dimension-agnostic. We emphasize, however, that any method that orders points in a way that concentrates information near the diagonal of $\tilde{\Sigma}$ and justifies the low-rank approximation of off-diagonal blocks is suitable, such as ordering points according to a Hilbert space-filling curve or Z-ordering (Kamel & Faloutsos 1993).

Writing $\boldsymbol{\theta}_{-0}$ for all components of $\boldsymbol{\theta}$ other than the scale parameter θ_0 , the minimizer of $-l_H(\theta_0, \boldsymbol{\theta}_{-0})$ for fixed $\boldsymbol{\theta}_{-0}$ as a function of θ_0 is $\hat{\theta}_0(\boldsymbol{\theta}_{-0}) = n^{-1} \mathbf{y}^T \Sigma(1, \boldsymbol{\theta}_{-0})^{-1} \mathbf{y}$. Thus, the negative log-likelihood can be minimized by instead minimizing the negative *profile log-likelihood*, given by

$$-l_{H,\text{pr}}(\boldsymbol{\theta}_{-0}) = -l_H(\hat{\theta}_0(\boldsymbol{\theta}_{-0}), \boldsymbol{\theta}_{-0}) = \frac{1}{2} \log |\tilde{\Sigma}(1, \boldsymbol{\theta}_{-0})| + \frac{n}{2} \log \left(\mathbf{y}^T \tilde{\Sigma}(1, \boldsymbol{\theta}_{-0})^{-1} \mathbf{y} \right),$$

which reduces the dimension of the minimization problem by one parameter. Its derivatives and trace estimators follow similarly as for the full log-likelihood.

All the computations shown in this section were performed on a standard workstation with an Intel Core i7-6700 processor and 40 GB of RAM, and the assembly of $\tilde{\Sigma}$, $\tilde{\Sigma}_j$, and $\tilde{\Sigma}_{jk}$ is done in multicore parallel, as is the factorization of $\tilde{\Sigma} = \mathbf{W}\mathbf{W}^T$. A software package written in the Julia language, `KernelMatrices.jl`, which provides the source code to perform all the computations described in this paper as well as reproduce the results in this section, is available at bitbucket.org/cgeoga/kernelmatrices.jl.

3.1 Quasilinear scaling of the log-likelihood, gradient, and Hessian

To demonstrate the scaling of the approximated log-likelihood, its stochastic gradient, and its Hessian, we show in Figure 1 the average time taken to evaluate those functions for the two-parameter (fixing ν) full Matérn log-likelihood (as opposed to profile likelihood) for sizes $n = 2^k$ for k ranging from 10 to 18, including also the time taken to call the exact functions for $k \leq 13$.

As can be seen in Figure 1, the scaling of all three operations for the approximated log-likelihood follow the expected quasilinear $O(n \log^2 n)$ growth, if not scaling even slightly better. For practical applications, the total time required to compute these values together will be slightly lower than the sum of the three times plotted here because of repeated computation of the derivative matrices $\tilde{\Sigma}_j$, repeated linear solves of the form $\tilde{\Sigma}^{-1} \mathbf{y}$, and other micro-optimizations that combine to save computational effort.

3.2 Numerical accuracy of symmetrized trace estimation

To demonstrate the benefit of the symmetrized stochastic trace estimation described in the Introduction, we simulate a process at random locations in the domain $[0, 100]^2$ with

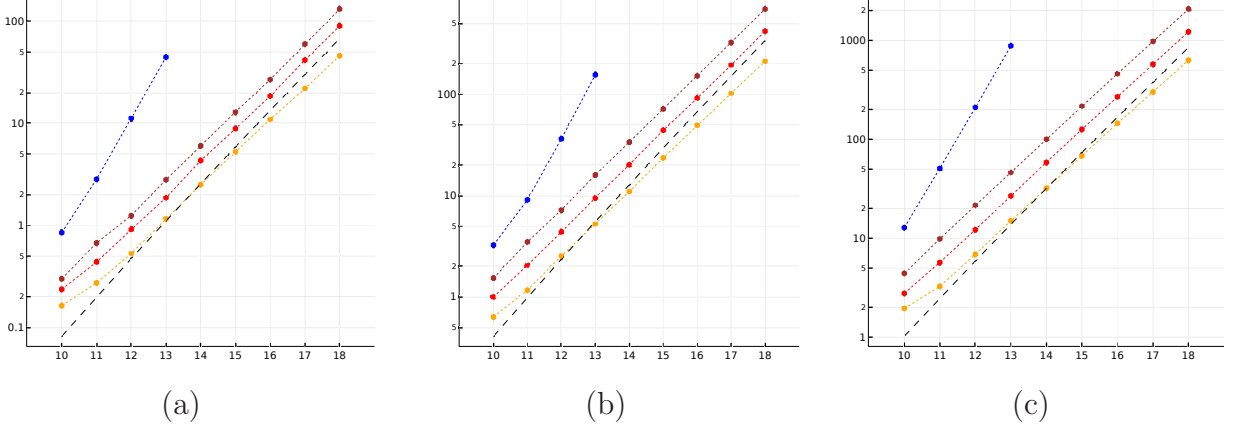


Figure 1: Times taken to call the likelihood (a), gradient (b), and Hessian (c) exactly (blue) and their HODLR equivalents for fixed off-diagonal rank 32 (orange), 72 (red), and 100 (brown) for sizes 2^k with k ranging from 10 to 18 (x-axis). Theoretical lines corresponding to $O(n \log^2 n)$ are added to each plot to demonstrate the scaling.

Matérn covariance with parameters $\theta_0 = 3$, $\theta_1 = 40$, and ν fixed at 1 and then compare the standard and symmetrized trace estimators for $\tilde{\Sigma}^{-1} \tilde{\Sigma}_j$ associated with θ_0 and θ_1 . We choose a large-range parameter with respect to the edge length of the domain in order to demonstrate that even for poorly conditioned $\tilde{\Sigma}$, the symmetrized trace estimator performs well. As the standard deviations shown in Figure 2 demonstrate, the symmetrized trace estimator reduces the standard deviation of estimates by more than a factor of 10. We also note the axes on Figure 2a, where n denotes *nano*. As remarked in the Introduction, for the scale parameter θ_0 , $\tilde{\Sigma}^{-1} \tilde{\Sigma}_j$ is a multiple of the identity matrix, so there is no stochastic error even for one \mathbf{u}_l , and the errors reported here are purely numerical.

3.3 Effect of method parameters on likelihood surface

Using the Matérn covariance function, we simulate $n = 2^{12}$ observations of a random field with Matérn covariance function with parameters $\theta_0 = 3.0$, $\theta_1 = 5.0$, and fixed $\nu = 1$ at random locations on the box $[0, 100]^2$. In Figure 3, which shows the log-likelihood surfaces for various levels with the minimizer of each subtracted off, we see the minimal effect on the location of the minimizer caused by varying the level of the HODLR approximation (with off-diagonal rank fixed at 64 for nonexact likelihoods). In the title of each subplot, we also show the value of the minimizer, demonstrating that as the level of the approximation varies the log-likelihood can see a substantial additive shift. To study the significance of the discrepancy in minimizing pixels in the displayed plots of the log-likelihood surfaces for different levels more quantitatively, we provide in Table 1 the numerical differences $|l(\hat{\boldsymbol{\theta}}) - l(\hat{\boldsymbol{\theta}}_k)|$ and $|l_H^{(k)}(\hat{\boldsymbol{\theta}}_k) - l_H^{(k)}(\hat{\boldsymbol{\theta}})|$, where $l_H^{(k)}$ denotes the approximated likelihood computed with $\tilde{\Sigma}$ having HODLR level k . We use $\hat{\boldsymbol{\theta}}_k$ to refer to the minimizing pixel of $l_H^{(k)}$.

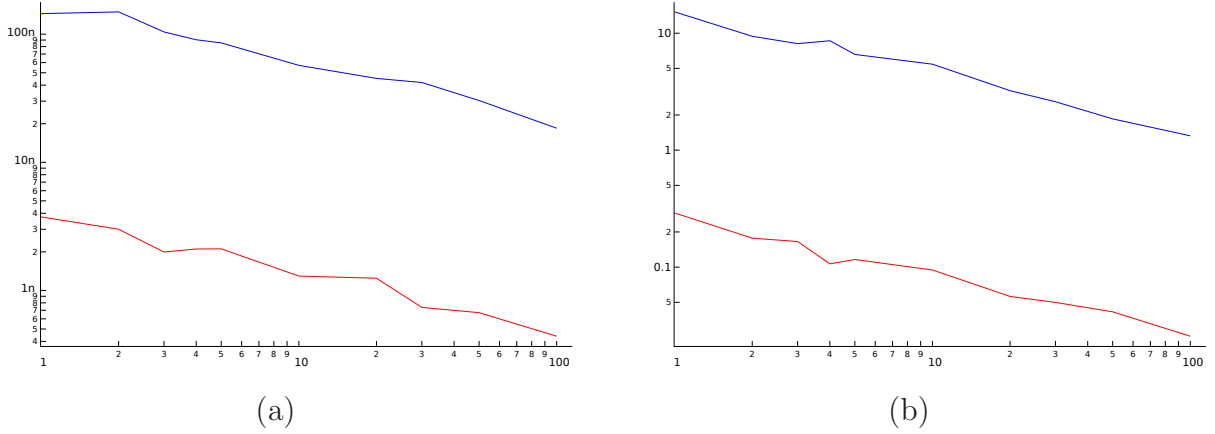


Figure 2: Standard deviation of 50 stochastic trace estimates for $\tilde{\Sigma}^{-1}\tilde{\Sigma}_j$ for the scale parameter (a) and range parameter (b) of the Matérn covariance. As can be seen, non-symmetrized estimates (blue) have standard deviations more than one order of magnitude larger than their symmetrized counterparts (red). The n in (a) denotes *nano*, so that 1n is 10^{-9} .

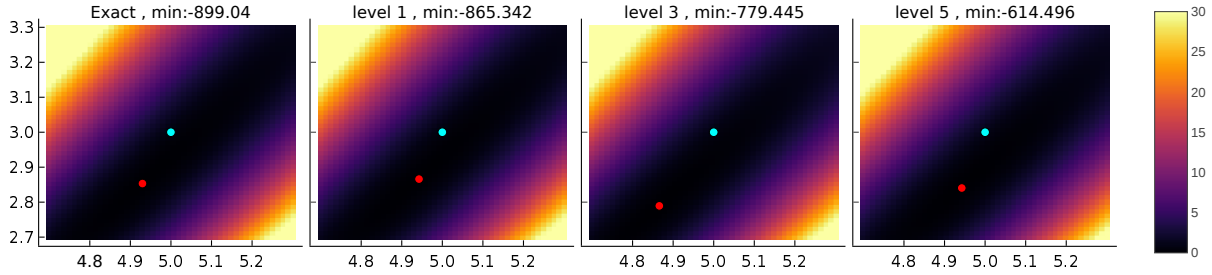


Figure 3: Centered log-likelihood surface for $n = 2^{12}$ data points randomly sampled on the box $[0, 100]^2$ with Matérn covariance with parameters $\theta_0 = 3$, $\theta_1 = 5$, and $\nu = 1$, with ν assumed known. The blue dot is the “true” parameters of the simulation, and the red dot is the minimizing pixel. The minimum value is shown with the level in the title.

Table 1: Absolute difference comparison of the log-likelihood at minimizers $\hat{\theta}_k$ for various levels k of the $\tilde{\Sigma}$ used to compute $-l_H$, with the minimizer of the exact likelihood, using $\hat{\theta}_k$ to denote the minimizing pixel of $l_H^{(k)}$.

	exact	$k = 1$	$k = 2$	$k = 3$	$k = 4$	$k = 5$
$ l(\hat{\theta}) - l(\hat{\theta}_k) $	0.0	0.0001	0.0	0.043	0.044	0.099
$ l_H^{(k)}(\hat{\theta}_k) - l_H^{(k)}(\hat{\theta}) $	0.0	0.001	0.0	0.037	0.030	0.054

As can be seen in Table 1, the largest difference is about 0.1, indicating that the minimizer for any level is reasonably close to the minimizer of the exact likelihood and vice versa. In Table 2, we provide the same analysis with fixed level 4 but varied off-diagonal ranks, where now $l_H^{(k)}$ refers to l_H being computed with a HODLR matrix of level 4 and fixed off-diagonal rank of k . Again, we see that the minimizers obtained for a wide variety of off-diagonal ranks are similar. In both tables, a value of 0.0 implies that the two minimizers were at the same pixel on the two-dimensional grid with an approximate step size of 0.01.

Table 2: Absolute difference comparison of the log-likelihood at minimizers $\hat{\boldsymbol{\theta}}_k$ for various fixed off-diagonal ranks k with the minimizer of the exact likelihood, where $\hat{\boldsymbol{\theta}}_k$ denotes the minimizing pixel of $l_H^{(k)}$.

	exact	$k = 2$	$k = 36$	$k = 48$	$k = 72$	$k = 96$
$ l(\hat{\boldsymbol{\theta}}) - l(\hat{\boldsymbol{\theta}}_k) $	0.0	0.123	0.038	0.038	0.125	0.038
$ l_H^{(k)}(\hat{\boldsymbol{\theta}}_k) - l_H^{(k)}(\hat{\boldsymbol{\theta}}) $	0.0	0.057	0.036	0.074	0.087	0.053

We can deduce from these experiments that while the magnitude of the log-likelihood certainly varies with the level and off-diagonal rank, making it potentially inappropriate to compare log-likelihood values across models, the minimizers agree in all scenarios to a decent degree. This agreement suggests that results from fitting data should be at least somewhat robust and insensitive to the choice of level and off-diagonal rank and that those parameters are at least partially free to be chosen based on other computational concerns.

3.4 Numerical accuracy of stochastic derivative approximations

To elucidate the asymptotic behavior of the minimizers of $-l_H$, we now switch to a different parameterization of the Matérn covariance inspired by Stein (1999) and Zhang (2004), given by

$$K_s(\mathbf{x}, \mathbf{y}; \boldsymbol{\theta}, \nu) := \theta_0 \left(\frac{\theta_1}{2\sqrt{\nu}} \|\mathbf{x} - \mathbf{y}\| \right)^\nu \mathcal{K}_\nu \left(\frac{2\sqrt{\nu}}{\theta_1} \|\mathbf{x} - \mathbf{y}\| \right). \quad (10)$$

The advantage of this parameterization is that, unlike in (9), it clearly separates parameters that can be estimated consistently as the sample size grows on a fixed domain from those that cannot (Stein 1999, Zhang 2004, Zhang & Zimmerman 2005). Specifically, for bounded domains in 3 or fewer dimensions, results on equivalence and orthogonality of Gaussian measures suggest that both θ_0 and ν can be estimated consistently under the parameterization (10), whereas θ_0 cannot be estimated consistently under (9). The range parameter θ_1 cannot be estimated consistently under either parameterization.

To demonstrate the accuracy of the stochastic gradient and Hessian estimates of $-l_H$ with this covariance function, we compare them with the exact gradient and Hessian of the approximated log-likelihood computed directly for a variety of small sizes. For the specific setting of the computations, we simulate Gaussian process data at random locations on

the domain $[0, 100]^2$ with parameters $\boldsymbol{\theta} = (3, 5)$ and ν fixed at 1 to avoid the potentially confounding numerical difficulties of computing $\frac{\partial}{\partial \nu} \mathcal{K}_\nu(x)$.

To explore the numerical accuracy of the stochastic approximations, we consider both estimates at the computed MLE $\widehat{\boldsymbol{\theta}}$ and at a potential starting point for optimization, which was chosen to be $\boldsymbol{\theta}_{\text{init}} = (2, 2)$. For both cases, we consider the standard relative precision metric. We note, however, that if $-l_H$ were exactly minimized, its gradient would be exactly 0 and the relative precision would be undefined. Thus, we also consider the alternative measures of accuracy at the evaluated MLE given by $\eta_g := \|\widehat{\nabla l_H(\boldsymbol{\theta})} - \nabla l_H(\boldsymbol{\theta})\|_{\mathcal{I}(\boldsymbol{\theta})^{-1}}$ for the gradient and

$$\eta_{\mathcal{I}} := \text{tr} \left\{ (\widehat{\mathcal{I}}(\boldsymbol{\theta}) - \mathcal{I}(\boldsymbol{\theta})) (\mathcal{I}(\boldsymbol{\theta})^{-1} - \widehat{\mathcal{I}}(\boldsymbol{\theta})^{-1}) \right\}^{1/2}$$

for the expected Fisher matrix. These measures of precision are stable at the MLE and are invariant to all linear transformations; $\eta_{\mathcal{I}}$ is a natural metric for positive definite matrices in that, for fixed positive definite \mathcal{I} , it tends to infinity as a sequence of positive definite $\widehat{\mathcal{I}}$ tends to a limit that is only positive semidefinite. Using ε to denote the standard relative precision, Tables 3 and 4 summarize these results.

Table 3: Average relative precision (in \log_{10}) of the stochastic gradient and Hessian of the approximated log-likelihood for 5 simulations with $\boldsymbol{\theta} = (2, 2)$.

	$n = 2^{10}$	$n = 2^{11}$	$n = 2^{12}$	$n = 2^{13}$
$\varepsilon_{\widehat{\nabla l_H(\boldsymbol{\theta})}}$	-3.78	-3.46	-3.51	-3.60
$\varepsilon_{\widehat{Hl_H(\boldsymbol{\theta})}}$	-4.22	-3.89	-3.71	-3.79

Table 4: Average precisions (in \log_{10}) of the stochastic gradient, expected Fisher matrix, and Hessian at $\widehat{\boldsymbol{\theta}}$.

	$n = 2^{10}$	$n = 2^{11}$	$n = 2^{12}$	$n = 2^{13}$
$\varepsilon_{\widehat{\nabla l_H(\boldsymbol{\theta})}}$	-0.62	-1.42	-0.98	-1.75
$\varepsilon_{\widehat{Hl_H(\boldsymbol{\theta})}}$	-2.37	-1.86	-2.13	-2.04
η_g	-0.92	-0.93	-0.73	-0.96
$\eta_{\mathcal{I}}$	-1.77	-1.82	-1.86	-2.21

For the relative precision, the interpretation is clear: the estimated gradient and Hessian at $\boldsymbol{\theta} = (2, 2)$ have relative error less than 0.03%, which we believe demonstrates their suitability for numerical optimization. Near the MLE, the gradient estimate in particular can become less accurate, meaning that stopping conditions in minimization like $\|\widehat{\nabla l_H(\boldsymbol{\theta})}\| < \varepsilon_{\text{tol}}$ may not be suitable, for example, and that if the gradient is sufficiently small, even the signs of the terms in the estimate may be incorrect, which can be confounding for numerical optimization. Nonetheless, in later sections we demonstrate the ability to optimize to the relative tolerance of 10^{-8} in the objective function.

3.5 Simulated data verifications

Using the alternative parameterization of the Matérn covariance function with fixed $\nu = 1$ to denote a process that is just barely not mean-square differentiable, we simulate five datasets of size $n = 2^{18}$ on an even grid across the domain $[0, 100]^2$ using the *R* software *RandomFields* of Schlather et al. (2015); and we then fit successively larger randomly subsampled datasets (obtaining both point estimates and approximate 95% confidence intervals via the expected Fisher information matrix) from each of these of sizes 2^k for k ranging from 11 to 17, thus working exclusively with irregularly sampled data. We do this for two range parameters of $\theta_1 = 5$ and $\theta_1 = 50$ to further demonstrate the method’s flexibility, optimizing in the weak correlation case with a simple trust-region method that exactly solves the subproblem as described in Nocedal & Wright (2006) and with the implementation of the *method of moving asymptotes* provided by the NLOpt library (Johnson) in the strongly correlated case. In both circumstances, the stopping condition is chosen to be a relative tolerance of 10^{-8} . For $k \leq 13$, we provide parameters fitted with the exact likelihood to the same tolerance for comparison. Figures 4 and 5 summarize the results.

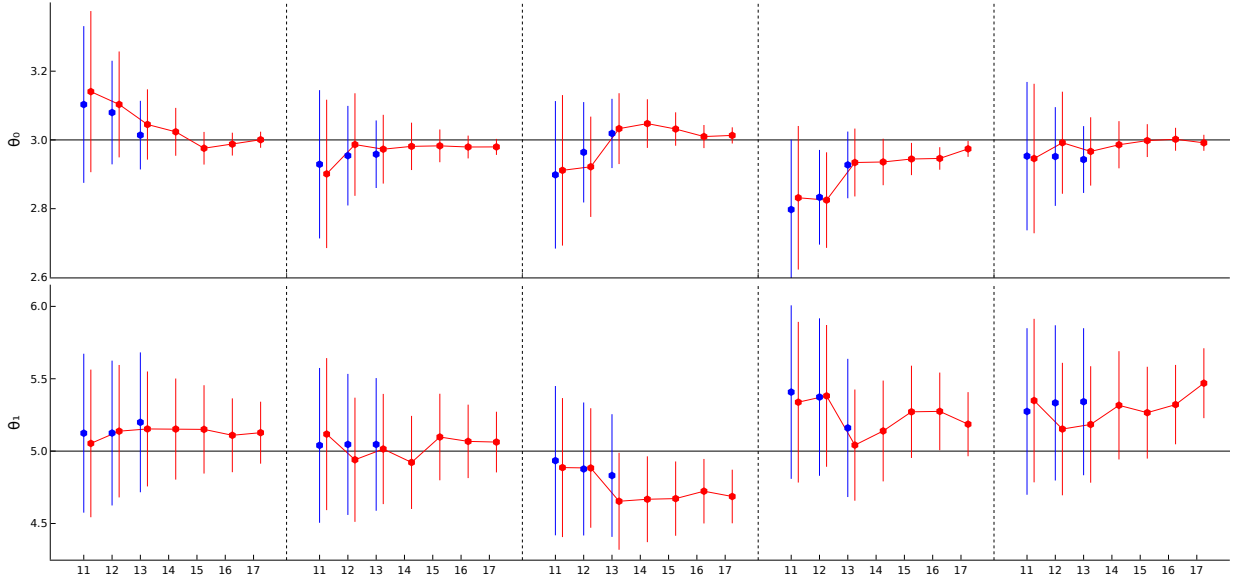


Figure 4: Estimated MLEs and confidence intervals for random subsamplings of 5 exactly simulated datasets of size $n = 2^{18}$ with covariance given by Equation 10 and parameters $\theta = (3, 5)$ and $\nu = 1$, with subsampled sizes 2^k with k ranging from 11 to 17 (x-axis).

The main conclusion from these simulations is that the minimizers of $-l_H$ closely resemble those of the exact log-likelihood and that the widths of the confidence intervals based on the approximate method are fairly close to those for the exact method. Assuming that this degree of accuracy applies to the larger sample sizes for which we were unable to do exact

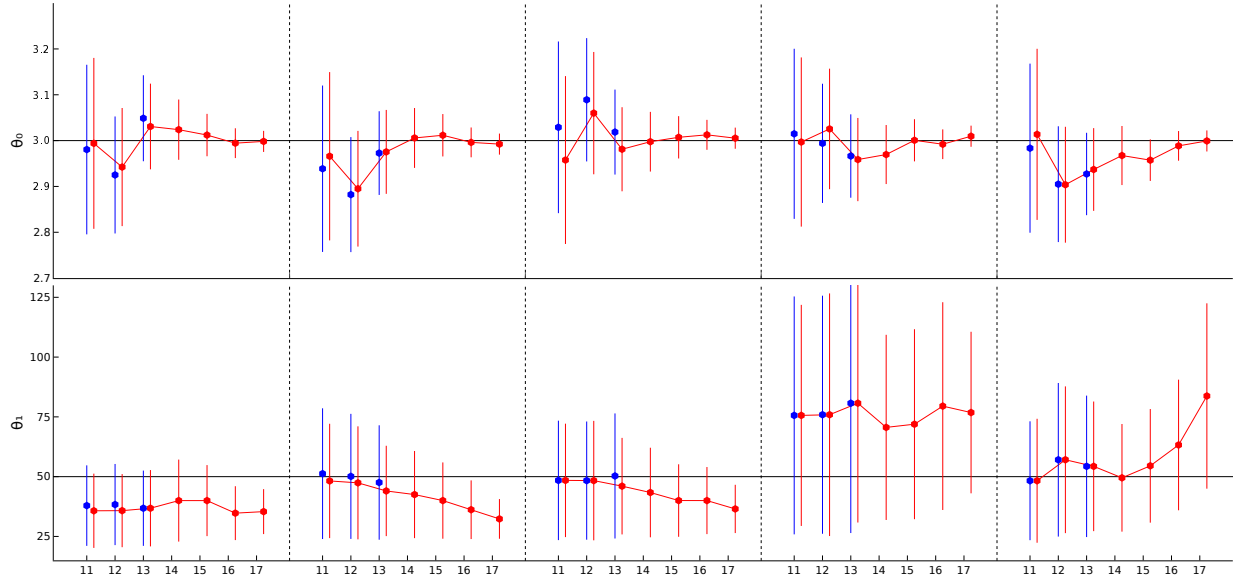


Figure 5: Same as Figure 4 except now with a large range parameter of $\theta_1 = 50$.

calculations, we see some interesting features in the behavior of the estimates as we take larger subsamples of the initial simulations of 2^{18} gridded observations. Specifically, we see that the estimates of the scale θ_0 continue to improve as the sample size increases, whereas, especially when the true range is 50, the estimated ranges do not obviously improve at the larger sample sizes, as is correctly represented in the almost constant widths of the confidence intervals for these larger sample sizes. These results are in accord with what is known about fixed-domain asymptotics for the Matérn model (Stein 1999, Zhang 2004, Zhang & Zimmerman 2005). We note that the asymptotic results underlying the use of Fisher information for approximate confidence intervals for MLEs, which includes consistency of the point estimates, are not valid in this setting. Nevertheless, the Fisher information matrix still gives a meaningful measure of uncertainty in the parameter estimates since it corresponds to the Godambe information matrix of the score equations (Heyde 2008). Additionally, these results demonstrate that the stochastic gradient and Hessian estimates are sufficiently stable even near the MLE and that numerical optimization to a relative tolerance of 10^{-8} can be performed.

4 Discussion

In this paper, we present an approximation of the Gaussian log-likelihood that can be computed in quasilinear time and admits both a gradient and Hessian with the same complexity, none of which requires selecting a preconditioner (which can be difficult; see Stein et al. (2013)). In the Numerical results section, we demonstrate that with the exact deriva-

tives of our approximated covariance matrices and the symmetrized trace estimation we can obtain very stable and performant estimators for the gradient and Hessian of the approximated log-likelihood and the expected information matrix. Further, we demonstrate that the minimizers of our approximated likelihood are nearly identical to the minimizers of the exact likelihood for a wide variety of method parameters and that the expected information matrix and the Hessian of our approximated likelihood are relatively close to their exact values. Putting these together, we present a coherent model for computing approximations of MLEs for Gaussian processes in quasilinear time that is kernel-independent and avoids many problem-specific computing challenges (such as choosing preconditioners). Further, the approach we advocate here (and the corresponding software) is flexible, making it an attractive and fast way to do exploratory work.

In some circumstances, however, our method is potentially less useful. The primary novel contribution of this method—an approximation strategy for covariance matrices Σ that facilitates the exact computation of the derivatives of the approximation as opposed to combining individual approximations of Σ and its derivatives—requires first partial derivatives of the kernel function with respect to the parameters. For simpler models as have been discussed here, this requirement is not problematic. For some covariance functions, however, these derivatives may need to be computed with the aid of automatic differentiation (AD) or even finite differencing (FD). This issue comes up even with the Matérn kernel, since, to the best of our knowledge, no usable code exists for efficiently computing the derivatives $\frac{\partial^k}{\partial \nu^k} \mathcal{K}_\nu(x)$ analytically, even though series expansions for these derivatives are available (see 10.38.2 and 10.40.8 in Olver et al. (2010)). Empirically, we have obtained reasonable estimates for $\hat{\nu}$ using finite difference approximations for these derivatives when ν is small. The main difficulty with finite differencing, however, is that it introduces a source of error that is hard to monitor, so that it can be difficult to recognize when estimates are being materially affected by the quality of the finite difference approximations. While the algorithm will still scale with the same complexity if AD or FD is used as a substitute for exactly computed derivatives, doing so will likely introduce a serious fixed overhead cost as well as potential numerical error in the latter case. With that said, however, the overhead will be incurred during the assembly stage, which is particularly well-suited to extreme parallelization that may mitigate such performance concerns.

Another circumstance in which this method may not be the most suitable is one where very accurate trace estimation is required, such as optimizing to a very high precision. As has been discussed, the peeling method of Lin et al. (2011) may be used, but matvec actions with the derivative matrices, especially $\tilde{\Sigma}_{jk}$, have a very high overhead, which may make the peeling method unacceptably expensive. Parallelization would certainly also mitigate this cost, but the fact remains that performing $O(\log n)$ many matvecs with $\tilde{\Sigma}_{jk}$ will come at a significant price.

Moreover, in some circumstances the framework of hierarchical matrices may be categorically less appropriate, or at least would need to be applied with care. It has been shown that, at least in some cases, as the dimension of a problem increases or its geometry changes, the numerical rank of the low-rank blocks of kernel matrices will increase

(Ambikasaran et al. 2016), which will affect the scaling of the algorithms that attempt to control pointwise precision. For algorithms that do not attempt to control pointwise precision, such as the one presented here, the complexity will not change, but the quality of the approximation will deteriorate. Moreover, off-diagonal blocks of kernel matrices often have low numerical rank because the corresponding kernel is smooth away from the origin (Ambikasaran et al. 2016). For covariance kernels for which this does not hold, off-diagonal blocks may not be of low numerical rank regardless of the dimension or geometry of the problem. For most standard covariance functions in spatial and space-time statistics, there is analyticity away from the origin. And most space-time processes happen in a dimension of at most four, so the problems of dimensionality may not often be encountered. But for some applications, for example in machine learning, that are done in higher dimensions, we suggest using care to be sure that the theoretical motivations for this approximation hold to a reasonable degree.

Acknowledgments

This material was based upon work supported by the U.S. Department of Energy, Office of Science, Office of Advanced Scientific Computing Research (ASCR) under Contracts DE-AC02-06CH11347 and DE-AC02-06CH11357. We acknowledge partial NSF funding through awards FP061151-01-PR and CNS-1545046 to MA.

References

- Ambikasaran, S. & Darve, E. (2013), ‘An $O(n \log n)$ fast direct solver for partially hierarchically semi-separable matrices’, *Journal of Scientific Computing* **57**(3), 477–501.
- Ambikasaran, S., O’Neil, M. & Singh, K. (2016), ‘Fast symmetric factorization of hierarchical matrices with applications’.
URL: <https://arxiv.org/abs/1405.0223v2>
- Ambikasaran, S., Foreman-Mackey, D., Greengard, L., Hogg, D. & O’Neil, M. (2016), ‘Fast direct methods for Gaussian processes’, *IEEE transactions on pattern analysis and machine intelligence* **38**(2), 252–265.
- Anitescu, M., Chen, J. & Wang, L. (2011), ‘A matrix-free approach for solving the parametric Gaussian process maximum likelihood problem’, *SIAM J. Sci. Comput.* **34**(1), 240–262.
- Bebendorf, M. (2000), ‘Approximation of boundary element matrices’, *Numerische Mathematik* **86**(4), 565–589.
- Bebendorf, M. & Hackbusch, W. (2007), ‘Stabilized rounded addition of hierarchical matrices’, *Numerical Linear Algebra with Applications* **14**(5), 407–423.

- Börm, S. & Garcke, J. (2007), Approximating Gaussian processes with H2-matrices, in ‘European Conference on Machine Learning’, pp. 42–53.
- Caragea, P. & Smith, R. (2007), ‘Asymptotic properties of computationally efficient alternative estimators for a class of multivariate normal models’, *Journal of Multivariate Analysis* **98**(7), 1417–1440.
- Castrillon-Candas, J., Genton, M. & Yokota, R. (2016), ‘Multi-level restricted maximum likelihood covariance estimation and kriging for large non-gridded spatial datasets’, *Spatial Statistics* **18**, 105–124.
- Chen, J. & Stein, M. (2017), ‘Linear-cost covariance functions for Gaussian random fields’.
URL: <https://arxiv.org/abs/1711.05895>
- Cressie, N. & Johannesson, G. (2006), ‘Spatial prediction for massive datasets’, *Proceedings of the Australian Academy of Science, Elizabeth and Frederick White Conference* pp. 1–11.
- Drineas, P. & Mahoney, M. (2005), ‘On the nyström method for approximating a gram matrix for improved kernel-based learning’, *J. Mach. Learn. Res.* **6**, 2153–2175.
- Efron, B. & Hinkley, D. (1978), ‘Assessing the accuracy of the maximum likelihood estimator: Observed versus expected Fisher information’, *Biometrika* **65**.
- Furrer, R., Genton, M. & Nychka, D. (2006), ‘Covariance tapering for interpolation of large spatial datasets’, *Journal of Computational and Graphical Statistics* **15**(3), 502–523.
- Godambe, V. (1991), *Estimating functions*, Oxford University Press.
- Grasedyck, L. & Hackbusch, W. (2003), ‘Construction and arithmetics of H-matrices’, *Computing* **70**(4), 295–334.
- Griewank, A. & Walther, A. (2008), *Evaluating derivatives: principles and techniques of algorithmic differentiation*, Vol. 105, SIAM.
- Hackbusch, W. (1999), ‘A sparse matrix arithmetic based on H-matrices, Part I: Introduction to H-matrices’, *Computing* **62**(2), 89–108.
- Hackbusch, W. (2015), *Hierarchical Matrices: Algorithms and Analysis*, Springer.
- Heyde, C. (2008), *Quasi-likelihood and its application: a general approach to optimal parameter estimation*, Springer Science & Business Media.
- Hutchinson, M. (1990), ‘A stochastic estimator of the trace of the influence matrix for laplacian smoothing splines’, *Communications in Statistics – Simulation and Computation* **19**(2), 433–450.
- Johnson, S. (n.d.), ‘The NLOpt nonlinear-optimization package’.
URL: <http://ab-initio.mit.edu/nlopt>

- Kamel, I. & Faloutsos, C. (1993), Hilbert r-tree: An improved r-tree using fractals, Technical report.
- Katzfuss, M. (2017), ‘A multi-resolution approximation for massive spatial datasets’, *Journal of the American Statistical Association* **112**(517), 201–214.
- Katzfuss, M. & Guinness, J. (2018), ‘A general framework for Vecchia approximations of Gaussian processes’.
URL: <https://arxiv.org/abs/1708.06302>
- Kaufman, C., Schervish, M. & Nychka, D. (2008), ‘Covariance tapering for likelihood-based estimation in large spatial data sets’, *Journal of the American Statistical Association* **103**(484), 1545–1555.
- Lin, L., Lu, J. & Ying, L. (2011), ‘Fast construction of hierarchical matrix representation from matrix-vector multiplication’, *J. Comput. Phys.* **230**, 4071–4087.
- Lindgren, F., Rue, H. & Lindstrom, J. (2011), ‘An explicit link between Gaussian fields and Gaussian markov random fields: the stochastic partial differential equation approach’, *Journal of the Royal Statistical Society: Series B (Statistical Methodology)* **73**(4), 423–498.
- Litvinenko, A., Sun, Y., Genton, M. & Keyes, D. (2017), ‘Likelihood approximation with hierarchical matrices for large spatial datasets’.
URL: <https://arxiv.org/abs/1709.04419>
- Minden, V., Damle, A., Ho, K. & Ying, L. (2017), ‘Fast spatial Gaussian process maximum likelihood estimation via skeletonization factorizations’, *Multiscale Modeling & Simulation* **15**(4), 1584–1611.
- Nocedal, J. & Wright, S. (2006), *Numerical Optimization*, Springer Series in Operations Research and Financial Engineering, Springer New York.
- Olver, F., Lozier, D., Boisvert, R. & Clark, C. (2010), *NIST Handbook of Mathematical Functions*, Cambridge University Press.
- Rjasanow, S. (2002), Adaptive cross approximation of dense matrices, in ‘Proc Int Assoc Bound Elem Methods’.
- Rue, H. & Held, L. (2005), *Gaussian Markov random fields: theory and applications*, CRC press.
- Schlather, M., Malinowski, A., Menck, P., Oesting, M. & Strokorb, K. (2015), ‘Analysis, simulation and prediction of multivariate random fields with package RandomFields’, *Journal of Statistical Software* **63**(8), 1–25.
- Stein, M. (1999), *Interpolation of Spatial Data: Some Theory for Kriging*, Springer.

- Stein, M. (2014), ‘Limitations on low rank approximations for covariance matrices of spatial data’, *Spatial Statistics* **8**.
- Stein, M., Chen, J. & Anitescu, M. (2013), ‘Stochastic approximation of score functions for Gaussian processes’, *Ann. Appl. Stat.* **7**(2), 1162–1191.
- Stein, M., Chi, Z. & Welty, L. (2004), ‘Approximating likelihoods for large spatial data sets’, *Journal of the Royal Statistical Society Series B* **66**, 275–296.
- Sun, Y. & Stein, M. (2016), ‘Statistically and computationally efficient estimating equations for large spatial datasets’, *Journal of Computational and Graphical Statistics* **25**(1), 187–208.
- Vecchia, A. (1988), ‘Estimation and model identification for continuous spatial processes’, *Journal of the Royal Statistical Society. Series B (Methodological)* **50**(2), 297–312.
- Williams, C. & Seeger, M. (2001), Using the Nystrm method to speed up kernel machines, in ‘Advances in Neural Information Processing Systems 13’, MIT Press, pp. 682–688.
- Xia, J. & Gu, M. (2010), ‘Robust approximate Cholesky factorization of rank-structured symmetric positive definite matrices’, *SIAM J. Matrix Anal. Appl.* **31**(5), 2899–2920.
- Zhang, H. (2004), ‘Inconsistent estimation and asymptotically equal interpolations in model-based geostatistics’, *Journal of the American Statistical Association* **99**(465), 250–261.
- Zhang, H. & Zimmerman, D. (2005), ‘Towards reconciling two asymptotic frameworks in spatial statistics’, *Biometrika* **92**(4), 921–936.

<p>Government License: The submitted manuscript has been created by UChicago Argonne, LLC, Operator of Argonne National Laboratory (“Argonne”). Argonne, a U.S. Department of Energy Office of Science laboratory, is operated under Contract No. DE-AC02-06CH11357. The U.S. Government retains for itself, and others acting on its behalf, a paid-up nonexclusive, irrevocable worldwide license in said article to reproduce, prepare derivative works, distribute copies to the public, and perform publicly and display publicly, by or on behalf of the Government. The Department of Energy will provide public access to these results of federally sponsored research in accordance with the DOE Public Access Plan. http://energy.gov/downloads/doe-public-access-plan.</p>

A Exact expressions for $\tilde{\Sigma}_{jk}$

As described in Section 2, derivatives of off-diagonal block approximations in the form of (4) are given by (6). The Hessian of the approximated log-likelihood requires the second derivative of $\tilde{\Sigma}$, which in turn requires the partial derivatives of (6). Continuing with the same notation as in Section 2, three simple product rule computations show that the k th partial derivative of (6) is given by

$$\begin{aligned}
\tilde{\Sigma}_{j,k,(I,J)} &= \Sigma_{j,k,(I,P)} \Sigma_{P,P}^{-1} \Sigma_{P,J} \\
&\quad - \Sigma_{j,(I,P)} \Sigma_{P,P}^{-1} \Sigma_{k,(P,P)} \Sigma_{P,P}^{-1} \Sigma_{P,J} \\
&\quad + \Sigma_{j,(I,P)} \Sigma_{P,P}^{-1} \Sigma_{k,(P,J)} \\
&\quad + \Sigma_{k,(I,P)} \Sigma_{(P,P)}^{-1} \Sigma_{j,(P,P)} \Sigma_{P,P}^{-1} \Sigma_{P,J} \\
&\quad - \Sigma_{I,P} \Sigma_{(P,P)}^{-1} \Sigma_{k,(P,P)} \Sigma_{(P,P)}^{-1} \Sigma_{j,(P,P)} \Sigma_{P,P}^{-1} \Sigma_{P,J} \\
&\quad + \Sigma_{(I,P)} \Sigma_{(P,P)}^{-1} \Sigma_{j,k,(P,P)} \Sigma_{P,P}^{-1} \Sigma_{P,J} \\
&\quad - \Sigma_{I,P} \Sigma_{(P,P)}^{-1} \Sigma_{j,(P,P)} \Sigma_{(P,P)}^{-1} \Sigma_{k,(P,P)} \Sigma_{P,P}^{-1} \Sigma_{P,J} \\
&\quad + \Sigma_{(I,P)} \Sigma_{(P,P)}^{-1} \Sigma_{j,(P,P)} \Sigma_{P,P}^{-1} \Sigma_{k,(P,J)} \\
&\quad + \Sigma_{k,(I,P)} \Sigma_{P,P}^{-1} \Sigma_{j,(P,J)} \\
&\quad - \Sigma_{(I,P)} \Sigma_{k,(P,P)}^{-1} \Sigma_{k,(P,P)} \Sigma_{P,P}^{-1} \Sigma_{j,(P,J)} \\
&\quad + \Sigma_{(I,P)} \Sigma_{P,P}^{-1} \Sigma_{j,k,(P,J)}.
\end{aligned}$$

Although this expression looks unwieldy and expensive, each line is still expressible as the sum of rank p matrices that can be written as $\mathbf{U}\mathbf{S}\mathbf{V}^T$, where $\mathbf{S} \in \mathbb{R}^{p \times p}$, meaning that a matvec operation with the block shown above will still scale with linear complexity for fixed p . While the overhead involved is undeniably substantial, the assembly and application of $\tilde{\Sigma}_{jk}$ is nonetheless demonstrated to scale with quasilinear complexity.